Heliyon 10 (2024) e35682

Contents lists available at ScienceDirect

Heliyon

journal homepage: www.cell.com/heliyon

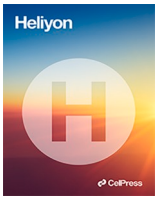

Research article

Enhancing water heater efficiency with aluminum and zinc-coated steel systems for energy solutions

Otong Nurhilal [a], Nur Muhammad Farizan [b], Fajrul Rahman [b], Setianto Setianto [a,*]

[a] Department of Physics FMIPA Padjadjaran University, Indonesia
[b] Study Program of Physics FMIPA Padjadjaran University, Jl. Raya Bandung-Sumedang KM.21 Jatinangor 45363, Sumedang, Jawa Barat, Indonesia

ARTICLE INFO

Keywords:
Solar collectors
Aluminum
Zinc-coated steel
Absorber
Efficiency

ABSTRACT

Solar collector plates are integral components for efficient solar heat transfer. While various metallic materials can serve as collector plates, aluminum stands out as a commonly employed choice with thermal conductivity comparable to copper and zinc. The material's thermal conductivity significantly impacts the heat transfer efficiency from sunlight to the collector. Moreover, the surface configuration of the plate is a crucial factor affecting solar heat absorption. This study investigates the utilization of corrugated collector plates made from two materials, aluminum and zinc-coated steel. The solar collector testing phase covers the dry and rainy seasons in Indonesia, thereby providing a comprehensive evaluation in various weather conditions. There are two stages of solar collector testing, namely testing before it is used to heat water and testing to heat water. Radiation data show seasonal variations, with higher radiation observed in the dry season. Evaluation of the performance of the solar collector before being used to heat water resulted in an average efficiency of 41.45 % for aluminum and 33.94 % for zinc-coated steel. Meanwhile, evaluation of the performance of solar collectors used to heat water produces an average efficiency of 20.40 % for aluminum and 10.47 % for zinc-coated steel. Corrugated aluminum solar collectors exhibited promising absorber potential, while zinc-coated steel demonstrated economic viability due to its lower cost compared to aluminum. The research underscores the potential applicability of solar collectors made from both materials throughout different seasons.

1. Introduction

Solar radiation represents a vast and renewable energy source, offering abundant and sustainable heat reservoirs on our planet. The direct conversion of solar energy into heat presents promising opportunities to meet the substantial demand for heat energy across industrial and residential sectors [1]. Harnessing solar energy holds the potential to significantly enhance heat energy provision in industries, catering to diverse needs such as water heating, steam generation, drying processes, cooling systems, air conditioning, desalination, and various applications within the food industry [2,3].

Research on solar collector systems in Indonesia has been conducted by researchers such as Syuhada et al. who conducted a study on the effect of iron absorber thickness for drying applications [4]. Andi et al. analyzed the performance of a solar water heating system

* Corresponding author.
E-mail address: setianto@phys.unpad.ac.id (S. Setianto).

https://doi.org/10.1016/j.heliyon.2024.e35682
Received 15 March 2024; Received in revised form 7 July 2024; Accepted 1 August 2024
Available online 2 August 2024

with a combination of absorber and phase change material (PCM) [5]. Dedy Ashari et al. conducted an experimental study on the effect of adding a reflector to flat plate collectors [6]. Nugroho et al. modified solar collectors from corrugated zinc with aluminum foil as an insulator [7].

Based on these research findings, in terms of materials used, heat absorbers are generally made from metals with high thermal conductivity, such as copper, aluminum, iron, steel, and zinc. To enhance solar radiation absorption, absorbers are coated with selective layers [8]. The difference in thermal conductivity values among various plate materials affects the heat absorption of the plates from the sun. Commonly used materials for collector plates include aluminum [9–12] and copper [13–15]. Solar collector plates made of aluminum exhibit higher efficiency compared to copper collector plates [9]. Although aluminum has lower thermal conductivity compared to copper, another metal, zinc, has lower thermal conductivity compared to aluminum and copper. However, modifying zinc as a solar collector plate is highly promising for development, considering that zinc is widely used as roofing material in mountainous regions in Indonesia. From the perspective of surface shape, flat plate solar collectors are the most popular because of their cost-effective design and ease of use in the solar collector field. They are typically used for medium-temperature applications such as water heaters and space heaters, making them popular in the domestic sector. Solar water heaters using flat plate collectors have become important in households due to their cost-effectiveness, offering significant advantages over conventional electric heaters by eliminating electricity costs. Although affordable and simple, flat plate collector efficiency faces challenges arising from higher heat transfer coefficients and less optimal thermal performance. Specifically, most heat losses, up to 75 %, occur from the top of flat plate collectors [16]. The overall performance of collectors depends on managing heat losses and optimizing optical properties within the system. Heat losses in flat plate collectors are influenced by factors such as the area of the glass cover, wind speed, and ambient temperature. In addition, if the solar collector is used to heat water, the position of the water pipe will affect the total heat loss from the solar collector. The position of the water pipe above the absorber provides a smaller total heat loss compared to the position of the water pipe below the absorber. Strategies to mitigate these losses include minimizing conductive-convective losses from the absorber plate to the glass cover, particularly at the top of the collector. It should be noted that flat plate collector efficiency tends to decrease with increasing wind loss coefficients [17]. Compared to flat plate solar collectors, Corrugated Solar Collectors (CSC) provide irradiation with scattered reflection, where the reflected light has varied angles, thus scattering light back to the surrounding absorber plate. This results in greater light absorption compared to flat plates [18]. This modification aims to enhance solar radiation absorption by the collector. Zhang et al.'s findings in 2018 showed that the height of the corrugated absorber is the most significant factor affecting collector performance [19]. Effective efficiency can reach 67.83 % with an air velocity of 1.14 m/s. Other experimental results show an efficiency of 60 % for a mass flow rate of 0.025 kg/s [20]. The CSC with a 60.0° opening angle achieve the highest useful energy and average thermal efficiency of 87.54 kWh and 82.31 %, respectively, outperforming flat plate solar collectors [18]. The research results show that corrugated surface solar collectors have a large heat transfer area and high heat transfer coefficients, making them suitable for use in rural buildings in cold regions [21]. The corrugated absorber is approximated to be a V-corrugated configuration to consider the radiative heat transfer due to its similar geometry and literature availability of radiative heat transfer correlations for V-corrugated absorber [18].

All of these studies were conducted in only one seasonal condition, so it is unknown about the opportunities for utilizing solar collectors for various applications that can be done in all seasons as in Indonesia, namely the dry season and the rainy season. The presence of two seasons in Indonesia results in different levels of solar radiation each month and also varies depending on the city's location above sea level. This research involves making corrugated plate solar collectors using aluminum and zinc plate materials. The type of zinc used in this research is zinc-coated steel. The selection of materials in our experimental design is based on the physical properties and performance of the materials in specific environmental conditions. For the dry season, aluminum was chosen due to its high thermal conductivity, allowing for effective heat distribution. This is particularly crucial during dry seasons when environmental temperatures can be significantly high, as the use of aluminum helps maintain the temperature of the materials and system more stable. On the other hand, for the rainy season, zinc-coated steel was selected for its cost efficiency. Zinc-coated steel is generally cheaper compared to several other materials, including aluminum. In conditions where materials are frequently exposed to rain, the use of zinc-coated steel can be a more economical choice while still providing adequate performance. Additionally, zinc-coated steel is commonly used as roofing material in areas with high rainfall. Comprehensive testing is carried out in two conditions: one without a water heater load and the other with a water heater load. This study also aims to determine the differences in solar collector performance in the two seasons commonly occurring in Indonesia, namely the dry season from April to October and the rainy season from October to April. Aluminum is used for solar collectors in the dry season, while zinc-coated steel is used in the rainy season. According to the Indonesian Central Bureau of Statistics, the use of zinc-coated steel for house roofs in Indonesia reaches 4.39 %, with the rest predominantly using tiles as house roofs. However, this zinc-coated steel material has not been developed into solar collectors for water heaters and other applications. Due to differences in time and materials used, correlation/relationship analysis between variables cannot be performed based on measurement results and calculated parameters. The analysis is done by comparing with research conducted by other researchers using various materials.

2. Experimental method

In order to evaluate the performance of corrugated solar collectors made of aluminum and zinc-coated steel as water heaters with the water pipe positioned above the absorber, an experiment will be conducted following these steps. Initially, both types of solar collectors will be constructed with identical dimensions to ensure a fair comparison. Subsequently, testing will be carried out to measure the total heat loss from each collector and compare their thermal efficiency. Furthermore, testing will be conducted on both collectors during both dry and rainy seasons to understand their performance in various environmental conditions. Additionally, both

collectors will be assessed without a load to determine their individual performance and also as water heaters using an equivalent load. The results of these tests will be analyzed to evaluate the collectors' performance during dry and rainy seasons, as well as their efficiency as water heaters.

2.1. Set-up experiment

To initiate the solar collector installation experiment, begin by preparing aluminum and zinc-coated steel plates measuring 100 cm in length, 80 cm in width, and 0.10 cm in thickness. Additionally, procure a transparent glass cover with a thickness of 0.22 cm, insulation with a thickness of 0.63 cm, and water pipes with a diameter of 1.24 cm and a length of 85 cm. Construct the solar collector by arranging the plates under the transparent glass cover at a tilt of 40°. The position of the water pipe is placed above the absorber plate, as shown in Fig. 1. Integrate the water pipe network into the solar collector system, connecting it to the cooling channel. Ensure the provision of a water source and a warm water reservoir, as illustrated in Fig. 2. During the testing phase with a water heater load, ensure the flow of water from the bottom surface to the top of the plate, adhering to the configuration shown in Fig. 1. Conduct the testing phase between 10:30 a.m. and 2:15 p.m. West Indonesia Time (WIB), gathering data during this period on solar radiation intensity, ambient air temperature, plate temperature, and inlet and outlet water temperatures. Utilize essential equipment such as solar power meter (Extech SP505 Pocket Solar Power Meter) and an infrared thermometer (Fluke 62 Max IR Thermometer). Perform data collection for radiation, environmental temperature, and collector plate temperature every 15 min at three designated times: in May (dry season in Indonesia) for aluminum corrugated solar collectors (ACSC) and in October (rainy season in Indonesia) for zinc-coated steel corrugated solar collectors (ZCSC). The research site is located in Jatinangor, Sumedang, West Java, with geographic coordinates of 6°55′12″ South Latitude and 107°46′22″ East Longitude. This meticulous setup and testing protocol aim to evaluate the performance of aluminum and zinc-coated steel in a solar collector system under specific conditions.

In Fig. 3, a plate lies beneath the transparent glass, possibly composed of aluminum or zinc-coated steel. The glass serves a dual purpose: shielding and allowing sunlight to penetrate, enabling the plate to absorb solar radiation effectively. Furthermore, the image illustrates the positioning of fluid pipes, crucial for circulating the heat transfer fluid. Whether placed above or below the plate, their arrangement can significantly influence the solar collector's operational efficiency. The visual depiction in Fig. 3 aids in understanding the configuration of the solar collector components, showcasing how sunlight enters through the glass to reach the plate and highlighting the placement of the fluid pipes. This understanding is pivotal for assessing the solar collector's performance in capturing and utilizing solar energy efficiently.

2.2. Measuring instruments

Solar radiation was measured using a solar power meter with an accuracy of approximately 3 %. The inlet and outlet temperatures of the collector, as well as the cover and ambient temperatures, were recorded using a digital infrared thermometer with an accuracy of ±1.5 °C. Additionally, a solar power meter was employed to measure the intensity of solar radiation, while an anemometer was used to determine wind speed. An uncertainty analysis of the efficiency of the CSC has been conducted, which relies on the variables outlined in Tables 2 and 3. The method described by Pambudi et al. [7] and J.P. Holman [22] was utilized to analyze errors related to the procedure outlined below. Let R be a function of the independent variables y_1, y_2, y_3, y_4, ……, y_n.

$$R = f(y_1, y_2, y_3, y_4, \ldots\ldots y_n) \tag{1}$$

Consider C_R represents the measured result uncertainty and X_1, X_2, X_3 …, X_n represent the uncertainties of independent variables y_1, y_2, y_3, …, y_n, respectively, the value of C_R can be calculated as follows:

$$C_R = \left[\left(X_1 \frac{\partial R_1}{\partial y_1} \right)^2 + \left(X_2 \frac{\partial R_2}{\partial y_2} \right)^2 + \left(X_3 \frac{\partial R_3}{\partial y_3} \right)^2 + \ldots + \left(X_n \frac{\partial R_n}{\partial y_n} \right)^2 \right] \tag{2}$$

(a) (b)

Fig. 1. The two configurations of the solar collector: (a) with the water pipe positioned under the plate, and (b) with the water pipe located above the plate.

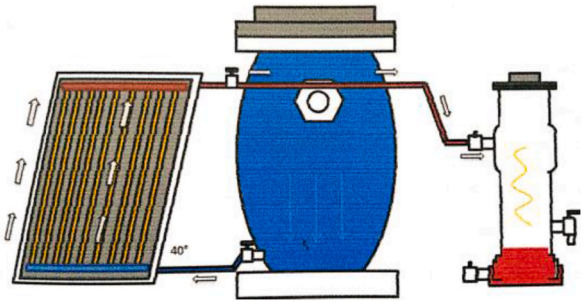

Fig. 2. The water pipe arrangement within the solar collector system.

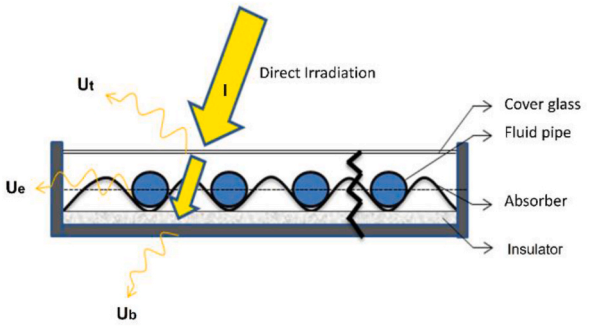

Fig. 3. The layout of the collector plate, cover glass, and the placement of the fluid pipe within the solar collector system.

The relative error E_{err} is presented below:

$$E_{err} = \frac{C_R}{R} \tag{3}$$

Referring to Tables 2 and 3, it can be estimated that the maximum relative error in the calculated energetic efficiency is approximately 3.9 %.

2.3. Experimental data

The experimental data collected during the study comprised a comprehensive array of variables, encompassing ambient temperature, solar radiation intensity, and water temperature before and after passing through the solar collector. Meanwhile, the data analysis involved the utilization of several equations established by Duffie and Beckman in 2013 [23]. Heat losses from different collector surfaces were computed using Equations (4)-(7)

$$U_L = U_t + U_b + U_e \tag{4}$$

$$U_t = \left[\frac{1}{h_w + h_{r,c-a}} + \frac{1}{h_{p-c} + h_{r,p-c}}\right]^{-1} \tag{5}$$

$$U_b = \frac{1}{\frac{k_b}{L_b} + \frac{2}{h_f}} \tag{6}$$

$$U_e = \frac{(UA)_{edge}}{A_c} \tag{7}$$

The corrugated shape of the solar collector absorber plate plays a significant role in determining the heat transfer from the sun to the absorber. The efficiency of the corrugated fin solar collector is enhanced because the reflections from the corrugated plate diffuse across other parts of the absorber plate. However, in this scenario, the radiation intensity received by the plate remains constant, allowing us to treat the plate as flat with a fin efficiency denoted as *F*. The calculation of fin efficiency is conducted using equations (8)–(11) as outlined by Fan et al. [24].

$$F = \frac{\tanh\sqrt{\frac{U_L}{k\delta}}\left(\frac{w-d}{2}\right)}{\sqrt{\frac{U_L}{k\delta}}\left(\frac{w-d}{2}\right)} \tag{8}$$

$$F' = \frac{1/U_L}{w\left[\frac{1}{U_L[d+(w-d)F]} + \frac{1}{\pi d h_f}\right]} \tag{9}$$

$$F'' = \frac{\dot{m}c_p}{A_c U_L F'}\left[1 - \exp\left(-\frac{A_c U_L F'}{\dot{m}c_p}\right)\right] \tag{10}$$

$$F_R = F'F'' \tag{11}$$

The heat removal factor (F_R) is a quantity that relates the actual delivered heat to the maximum possible heat. It is equivalent to the effectiveness of a conventional heat exchanger. The maximum possible heat gain in a solar collector occurs when the whole absorber is at the inlet fluid temperature. F' represents the fin factor efficiency, which is associated with the dimensions and geometry of the solar collector. This efficiency factor is crucial in determining how effectively the fins of the solar collector transfer heat, influenced by their size, shape, and arrangement within the collector. The heat dissipation coefficient depends on the area of the collector, the thermal loss coefficient, and the collector efficiency factor (F''). The absorbed useful heat, Q_u, by the collector plate and the collector efficiency can be expressed by equations (12) and (13) [25].

$$Q_u = A_c F_R[S - U_L(T_c - T_a)] \tag{12}$$

$$\eta_c = \frac{Q_u}{A_c I} \tag{13}$$

The efficiency of the absorber without a water heater load depends on the temperature absorbed by the absorber which is also influenced by the ambient temperature.

The heat source in the solar collector is solar energy, and its input power received by the collector surface is absorbed and then transferred to the working fluid. Fluid efficiency is calculated by dividing the fluid power by the input power from the collector. This efficiency is generally considered instantaneous efficiency because it is a function of momentary operating conditions, including local climate parameters such as ambient temperature, wind speed, etc [9,17]. The absorbed fluid energy efficiency is calculated using the following equation (14).

$$\eta_f = \frac{Q_f}{Q_u} \times 100\% \tag{14}$$

The energy used to heat the fluid is determined by recording the inlet and outlet water temperature data at a specific flow rate and subsequently calculated using equation (15) as follows

$$Q_f = \dot{m}C_p(T_o - T_i) \tag{15}$$

The total efficiency is then calculated by multiplying the collector efficiency by the fluid

$$\eta_t = \eta_c \times \eta_f \times 100\% \tag{16}$$

3. Results and discussion

The results of solar radiation measurements from 10:30 a.m. to 02:15 p.m. and the calculation of parameters for the corrugated flat plate solar collector are presented in Tables 4–7.

Based on the data extracted from Tables 4–7, the research data was collected between 10:30 a.m. to 2:15 p.m. local time (WIB). Specifically, during the rainy season and with the sun's position at latitudes south of the equator, a noticeable rise in solar radiation occurs at higher sun positions, followed by rainfall typically starting in the afternoon. This contrasts with the dry season, characterized by a gradual increase in sunlight from early morning until late afternoon. Utilizing data from both seasons, data processing was conducted within the timeframe of 10:30 a.m. to 2:15 p.m. to ensure a comprehensive analysis.

Table 1
Potential use of solar energy and material prices.

Solar energy potential		Material prices	
Solar radiation	4.8 kWh/m^2	Copper	IDR. 5,429,000 (1 mm × 1m x 1m)
PLTS	0.87 GW (2025)	Aluminum	IDR. 764,000 (per sheet)
Solar heater	–	Zinc-coated steel	IDR. 54,000 (per sheet)

PLTS = solar power plant.

Table 2
The ranges and accuracy of measurement devices.

Device	Measuring range	Accuracy
Thermometer IR	−30 to 500 °C	±1.5 °C
Solar power meter	0–4000 W/m^2	±3 %
Anemometer	1− 80 m/s	±2.5 %

Table 3
CSC system model description.

Specification	Dimension
Box Length	100 cm
Box Width	80 cm
Around the Box	360 cm
Square Area	80 cm^2
Top box thickness	3.70 cm
Thick bottom iron box	4.00 cm
Collector thickness	0.10 cm
Frame Width	3.00 cm
Glass Thickness	0.22 cm
Plate-to-Glass Distance	1.63 cm
Insulator thickness	0.62 cm
Glass transmittance	0.90
Plate absorbance thermal conductivity of aluminum	0.76
thermal conductivity of zinc-coated steel	237 W/mK
Thermal conductivity of air	60 W/mK
Styrofoam	0.0285 W/mK
Low water rate	0.03 W/mK
Thermal Diffusivity of air volumetric coefficient of air expansion	1.61 Lph
specific heat of water	1.9×10^{-5} m^2/s
Plate emittance	3.0×10^{-3}/K
Glass emittance	4200 J/kg K
	0.2
	0.8

Lph = liter per hour.

Table 4
Radiation data and parameters for the ACSC without a water heater load in dry season (May).

Time	I (W/m^2)	S (W/m^2)	U_L (W/m^{2}K)	T_c (^{o}C)	Q_u(W)	η_c (%)
10:30	716	544	9.3	52	273.51	38.20
10:45	750	570	9.32	53	293.44	39.12
11:00	789	600	9.36	53	316.01	40.05
11:15	785	597	9.4	50	327.71	41.75
11:30	779	592	9.4	51	316.77	40.66
11:45	751	571	9.41	50	307.30	40.92
12:00	762	579	9.44	49	320.81	42.10
12:15	753	572	9.44	49	315.45	41.89
12:30	725	551	9.42	49	306.43	42.27
12:45	721	548	9.41	49	304.18	42.19
13:00	669	508	9.4	48	273.33	40.86
13:15	672	511	9.39	48	275.25	40.96
13:30	662	503	9.38	45	284.14	42.92
13:45	646	491	9.29	44	275.66	42.67
14:00	605	460	9.24	42	259.06	42.82
14:15	586	445	9.09	41	256.52	43.77
Ave	**711**	**540**	**9.36**	**48.31**	**294.10**	**41.45**

Average value of $F_R = 0.98$.

The tests on solar radiation reveal a slight 5 % difference in average sunlight intensity between the dry season (711 W/m^2) and the rainy season (675 W/m^2). However, this small difference causes significant variations in solar collector efficiency for both absorber materials. In the dry season, when sunlight is stronger, materials like aluminum with high thermal conductivity (237 W/m.K) perform better. They absorb and transfer heat more efficiently, resulting in higher collector efficiency. In fact, with high thermal conductivity, aluminum's absorbent performance remains better, including during the rainy season. On the other hand, during the rainy season with slightly weaker sunlight, materials like zinc-coated steel with lower thermal conductivity (60 W/m.K), chosen for their cost-effectiveness and decent performance, still shows good performance. A techno-economic analysis would likely underscore zinc-

Table 5
Radiation data and parameters for the ACSC with a water heater load in dry season (May).

Time	$\dot{m}$ (Lph)	C_p (kJ/kg K)	T_{out} (°C)	T_{in} (°C)	Q_f (W)	η_f (%)	η_t (%)
10:30	1.61	4.2	50	27	155.53	56.86	21.72
10:45	1.61	4.2	52	27	169.05	57.61	22.54
11:00	1.61	4.2	54	27	182.57	57.77	23.14
11:15	1.61	4.2	53	27	175.81	53.65	22.40
11:30	1.61	4.2	52	27	169.05	53.37	21.70
11:45	1.61	4.2	50	28	148.76	48.41	19.81
12:00	1.61	4.2	50	28	148.76	46.37	19.52
12:15	1.61	4.2	50	28	148.76	47.16	19.76
12:30	1.61	4.2	48	28	135.24	44.13	18.65
12:45	1.61	4.2	48	28	135.24	44.46	18.76
13:00	1.61	4.2	47	28	128.48	47.00	19.20
13:15	1.61	4.2	47	27	135.24	49.13	20.13
13:30	1.61	4.2	46	27	128.48	45.22	19.41
13:45	1.61	4.2	46	27	128.48	46.61	19.89
14:00	1.61	4.2	45	27	121.72	46.98	20.12
14:15	1.61	4.2	44	27	114.95	44.81	19.62
Ave	**1.61**	**4.20**	**48.88**	**27.38**	**145.38**	**49.35**	**20.40**

Table 6
Radiation data and parameters for the ZCSC steel without a water heater load in rainy season (October).

Time	I (W/m^2)	S (W/m^2)	U_L (W/m^{2}K)	T_c (°C)	Q_u(W)	η_c (%)
10:30	592	458	14.00	40	225.33	38.06
10:45	629	487	15.58	43	217.77	34.62
11:00	666	515	15.30	46	213.66	32.08
11:15	671	519	14.50	48	214.14	31.91
11:30	687	532	14.20	49	230.74	33.59
11:45	735	569	14.00	49	249.54	33.95
12:00	754	584	14.50	49	262.24	34.78
12:15	765	592	14.40	49	265.74	34.74
12:30	768	594	14.00	50	273.30	35.59
12:45	759	587	14.00	55	199.78	26.32
13:00	723	560	14.50	52	202.27	27.98
13:15	671	519	14.40	50	180.70	26.93
13:30	663	513	14.30	46	221.82	33.46
13:45	599	464	14.00	41	235.28	39.28
14:00	564	437	14.20	39	222.01	39.36
14:15	550	426	14.20	38	222.42	40.44
Ave	**675**	**522**	**14.38**	**46.5**	**227.30**	**33.94**

Table 7
Radiation data and parameters for the ZCSC with a water heater load in rainy season (October).

Time	$\dot{m}$ (Lph)	C_p (kJ/kg K)	T_{out} (°C)	T_{in} (°C)	Q_f (W)	η_f (%)	η_t (%)
10:30	1.61	4.2	36	27	60.86	27.29	10.28
10:45	1.61	4.2	38	28	67.62	32.37	10.75
11:00	1.61	4.2	43	28	101.43	50.57	15.23
11:15	1.61	4.2	43	28	101.43	55.26	15.12
11:30	1.61	4.2	42	28	94.67	48.44	13.78
11:45	1.61	4.2	40	28	81.14	39.34	11.04
12:00	1.61	4.2	41	28	87.91	42.66	11.66
12:15	1.61	4.2	40	28	81.14	38.36	10.61
12:30	1.61	4.2	39	28	74.38	32.53	9.69
12:45	1.61	4.2	38	28	67.62	39.96	8.91
13:00	1.61	4.2	36	28	54.10	30.83	7.48
13:15	1.61	4.2	36	27	60.86	37.94	9.07
13:30	1.61	4.2	36	27	60.86	30.90	9.18
13:45	1.61	4.2	35	27	54.10	24.49	9.03
14:00	1.61	4.2	34	27	47.33	22.96	8.39
14:15	1.61	4.2	33	27	40.57	19.86	7.38
Ave	**1.61**	**4.20**	**38.47**	**27.67**	**73.03**	**36.93**	**10.47**

coated steel as a more economical choice in various applications due to its lower material costs, simpler manufacturing processes, comparable or superior durability, and favorable environmental credentials compared to aluminium.

A comprehensive analysis of the data presented in the tables was performed, and visual representations were created through plots for key parameters, as illustrated in Figs. 4–9.

In Fig. 4, the peak solar radiation of 789 W/m^2 was recorded at 11:00 a.m. in May, while at 12:30 p.m. in May, it was 768 W/m^2. These observations align with the seasonal patterns, with May representing the dry season in Indonesia and October representing the rainy season. The higher solar radiation during the dry season is consistent with the expectation of greater sunlight exposure, contributing to increased energy absorption by the solar collector.

In Figs. 5 and 6, the temperature measurements for the aluminum Corrugated Solar Collector (CSC) reveal notable trends. The collector temperature, representing the plate's surface temperature, reaches 53 °C, while the outlet temperature of the heated water reaches 54 °C. The average collector temperature is recorded at 48.31 °C, and the average outlet temperature is slightly higher at 48.88 °C. The substantial temperature difference of 21.5 °C between the average inlet and outlet temperatures indicates effective heat absorption by the collector. The drop efficiency from an average 41.45 % without water heating to 20.40 % with water heating for the ACSC (about 50 %). Contrastingly, for the ZCSC, the collector temperature reaches 55 °C, and the outlet temperature is slightly lower at 43 °C. The average collector temperature is 46.5 °C, and the average outlet temperature is notably lower at 38.47 °C. The temperature difference between the average inlet and outlet temperatures is 10.8 °C. The thermal conductivity of zinc-coated steel is about 60 W/m·K. This would also explain the drop of the zinc-coated steel absorber efficiency from an average of 33.94 % without water heating to 10.47 % with water heating (about 30 %). This suggests that the ACSC exhibits a lower temperature rise compared to the ACSC, indicating potential differences in heat absorption and transfer characteristics between the two materials.

Fig. 7 reveals significant insights into the comparative efficiency performance of the ACSC and ZCSC under no water heater load conditions. The data indicates that the ACSC outperforms the ZCSC in terms of both the highest and average efficiencies. Specifically, the ACSC achieves the highest efficiency of 43.77 % and an average efficiency of 41.45 %, while the ZCSC lags slightly with the highest efficiency of 39.36 % and an average efficiency of 33.94 %. This discrepancy suggests that the aluminum collector exhibits superior heat absorption and transfer capabilities, contributing to its overall higher efficiency. Fig. 8, which presents efficiency values under a water heater load, the superiority of the ACSC persists. The highest and average efficiencies for the aluminum collector are notably higher at 57.77 % and 49.25 %, respectively, compared to the ZCSC, which records a highest efficiency of 55.26 % and an average efficiency of 36.25 %. This underscores the advantageous thermal performance of the aluminum collector, particularly in scenarios with a water heater load.

In Fig. 9, the performance of ACSC and ZCSC collectors using their respective linear equations. From equations (12) and (13), the analysis reveals that the ACSC exhibits superior efficiency under ideal conditions, as indicated by its higher intercept of 39.279, although it experiences higher heat losses with a slope of 0.2551 as the temperature difference increases. In contrast, the ZCSC demonstrates lower maximum efficiency with an intercept of 32.825 but boasts better insulation, leading to lower heat losses with a less slope of 0.1315. Therefore, while ACSC is more efficient initially, ZCSC proves to be more effective at minimizing heat losses over varying temperature differences. Fig. 10 synthesizes the efficiency data, providing a comprehensive view of the average efficiency for collectors without heaters, collectors with heaters, and the total efficiency. This holistic analysis aids in understanding the overall performance of the solar collectors across different operational conditions, emphasizing the nuanced interplay between material composition and heat transfer efficiency.

Based on Tables 3 and 4, the total heat loss coefficient (U_L) serves as a cumulative measure of heat dissipation occurring at the upper, side, and lower parts of the solar collector, as depicted by Equations (1)–(4). The largest contribution to heat loss comes from the lower part of the collector (U_b), implying that the insulation material is insufficient in effectively retaining heat. The average U_L for the ACSC and ZCSC is 9.36 W/m^2 ^{o}C and 14.38 W/m^{2o}C, respectively. The average outlet water temperature for ACSC and ZCSC is

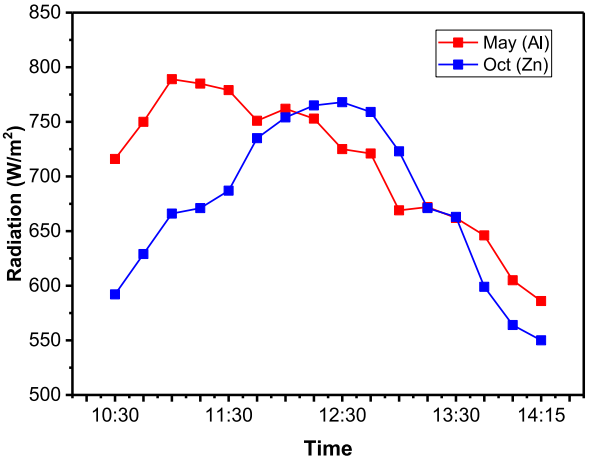

Fig. 4. Measured solar radiation as a function of time.

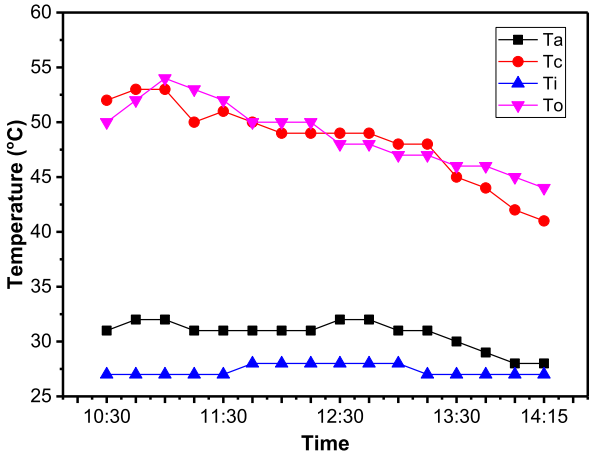

Fig. 5. Measured temperature as a function of time for aluminum solar collector.

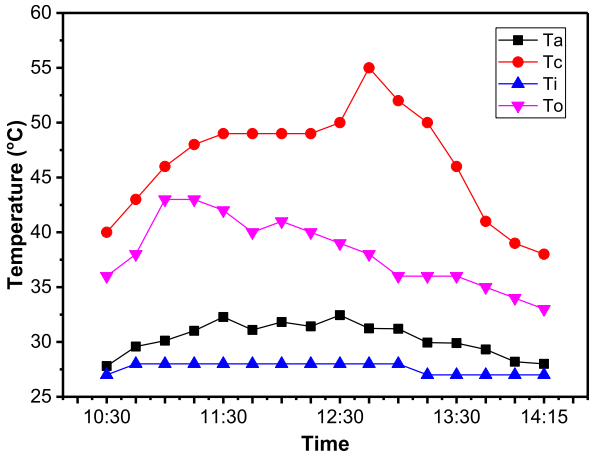

Fig. 6. Measured temperature as a function of time for zinc-coated steel solar collector.

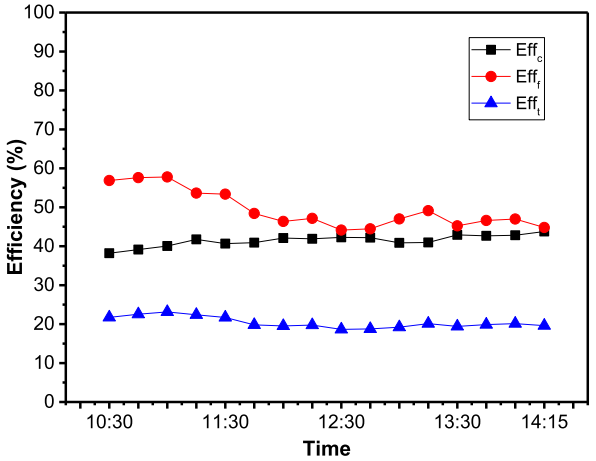

Fig. 7. Efficiency as a function of time of ACSC.

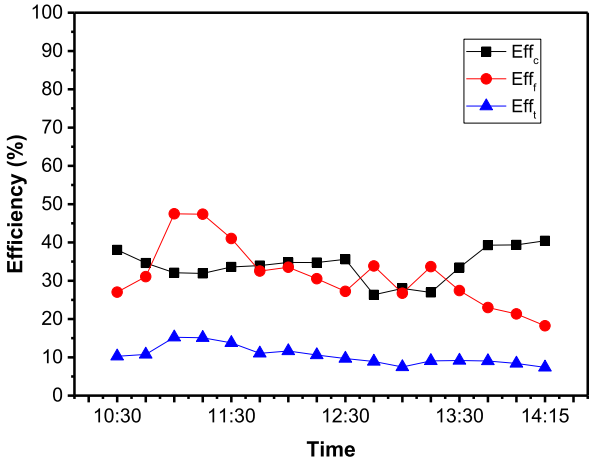

Fig. 8. Efficiency as a function of time of ZCSC.

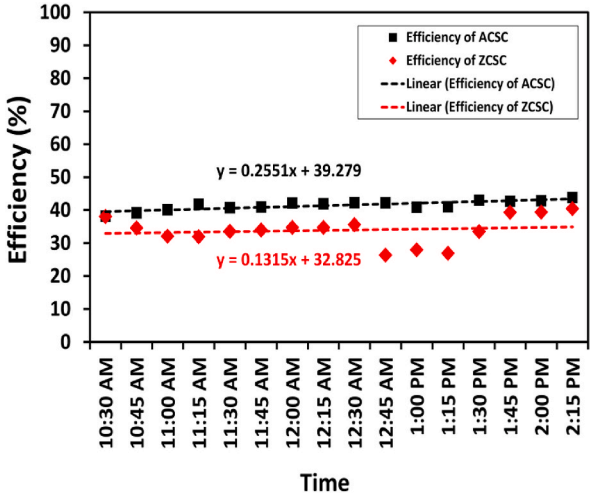

Fig. 9. Performance analysis of ACSC and ZCSC without a water heater load.

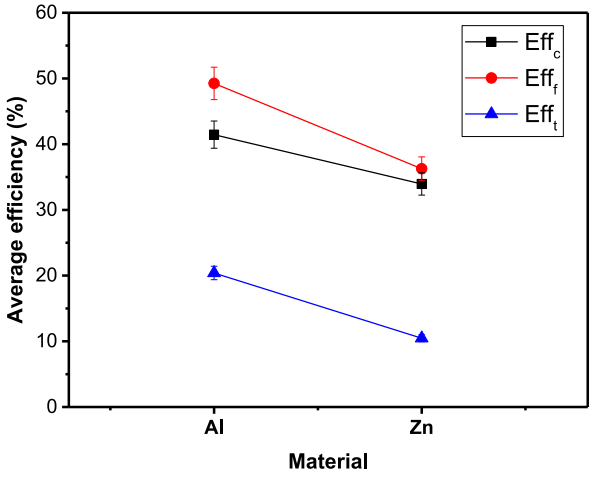

Fig. 10. Average efficiency of ACSC and ZCSC.

48.88 °C and 38.47 °C, respectively. This aligns with the condition that the surface temperature of ACSC is higher than ZCSC. A significant difference is observed in the average useful energy (Q_w) for ACSC and ZCSC after applying the water heating load, with values of 145.38 W and 73.03 W, respectively. The average efficiencies for ACSC and ZCSC are 20.40 % and 10.47 %, respectively. These values are consistent with the thermal conductivity of each plate. These results can be compared with findings from other studies on CSC made of aluminum. For instance, H. Vettrivel et al. used a single cover solar collector with $U_L = 5.3$ W/m^{2}K, $Q_w = 240$ Watts, and an efficiency of 63 % with the highest radiation reaching 946 W/m^2 [17]. Additionally, Dedy Ashari et al. reported $Q_w = 197.68$ W and an efficiency of 43.9 % with a flow rate of 20 L/h [6], featuring a corrugated type absorber. A. Sakhrieh et al. reported testing results for ACSC with an average efficiency of 59.3 % and the highest radiation reaching 1100 W/m^2 [9]. As for ZCSC reported efficiency values against fluid flow rates were 34 %/120 Lph, 40 %/180 Lph, and 50 %/240 Lph, with the highest solar radiation reaching nearly 1200 W/m^2. Based on Table 1, the utilization of solar energy in Indonesia is primarily focused on solar power plants in the form of solar panels (photovoltaic). Meanwhile, there is no valid data on the use of solar energy for water heaters. In economic terms, the use of aluminum as a solar collector is much more expensive compared to zinc-coated steel. Research conducted by Pambudi et al. suggests that zinc-coated steel holds promise as a highly cost-effective material for solar collectors [7].

4. Conclusion

Corrugated solar collectors made of aluminum and zinc-coated steel have been successfully made for water heaters with the water pipe positioned above the absorber. Although not significant, the total heat loss from the solar collector is reduced by positioning the water pipe above the absorber. Solar collector testing shows good results for each absorber material in different seasons. Good solar collector test results were also obtained from solar collectors with each material for testing without load for water heating and when used as a water heater. Based on the efficiency value of each material for each season, aluminum and zinc-coated steel can be recommended as absorbers. Economically, considering the significant price difference between aluminum and zinc-coated steel, it is recommended to use zinc-coated steel as an absorber with certain modifications.

Data availability

All data used for this study are contained in this article.

CRediT authorship contribution statement

Otong Nurhilal: Conceptualization, Methodology, Supervision, Writing – review & editing. **Nur Muhammad Farizan:** Data curation, Investigation, Validation. **Fajrul Rahman:** Resources, Investigation, Visualization. **Setianto Setianto:** Writing – original draft, Methodology, Formal analysis, Data curation.

Declaration of competing interest

The authors declare that they have no known competing financial interests or personal relationships that could have appeared to influence the work reported in this paper.

Acknowledgment

We would like to thank the energy physics laboratory of the physics department of Padjadjaran University.

Nomenclature

S	Absorbed radiation (W/m2)
I	Solar irradiation (W/m2)
L	Distance between plate and glass (m)
Le	Distance between edge and plate (m)
L_b	insulator thickness (m)
w	Distance between pipes (m)
d	Pipe outer diameter (m)
dh	Inner pipe diameter (m)
δ	Collector plate thickness (m)
δe	Thickness of the side box (m)
Nu	Nusselt number
NuD	Fluid Nusselt number
Ra	Rayleigh number
Re	Reynold number
T_p	Plate temperature (^{o}C)
T_c	Glass temperature (^{o}C)

T_s	Sky temperature (^oC)
T_a	Ambient temperature (^oC)
T_{in}	Inlet fluid temperatur (^oC)
T_{out}	Outlet fluid temperature (^oC)
F	Fin efficiency
F'	Fin efficiency factor
F''	Collector efficiency factor
F_R	Heat removal factor
U_L	Total heat loss coefficient (W/m^2K)
U_t	Top heat loss (W/m^2K)
U_e	Edge heat loss (W/m^2K)
U_b	Bottom heat loss (W/m^2K)
$\dot{m}$	Fluid flow rate (Lph)
A_c	Cross-sectional area of the collector plate (m^2)
V	Wind velocity (m/s)
K	Around the collector (m)
k_e	Edge conductivity (W/mK)
k_b	Insulator thermal conductivity (W/mK)
h_w	Wind convection coefficient (W/m^2K)
h	Heat transfer coefficient (W/m^2K)
h_f	Fluid convection coefficient (W/m^2K)
$h_{r,c\text{-}a}$	Glass-environment convection reflection coefficient (W/m^2K)
$h_{p\text{-}c}$	Glass-plate convection coefficient (W/m^2K)
$h_{r,p\text{-}c}$	Glass-plate convection reflection coefficient (W/m^2K)
Q_u	Useful energy solar collector (W)
Q_f	Useful energy of the fluid (W)

Greek letters

α	Absorptivity of collector, thermal diffusivity
ε	Emissivity
σ	Stefan-Boltzmann constant
τ	Transmissivity of glass
η	Efficiency
μ	Dynamic viscosity of fluids (kg/ms)

Subscripts

In	Inlet
Out	Outlet

References

[1] L. Kumar, et al., Prospects and challenges of solar thermal for process heating: a comprehensive review, Energies 15 (22) (2022) 8501.
[2] W. Strielkowski, et al., Renewable energy in the sustainable development of electrical power sector: a review, Energies 14 (24) (2021) 8240.
[3] A. Shokri, M.S. Fard, A sustainable approach in water desalination with the integration of renewable energy sources: environmental engineering challenges and perspectives, Environmental Advances 9 (2022) 100281.
[4] A. Syuhada, M.I. Maulana, Heat transfer capability of solar radiation in colored roof and influence on room thermal comfort, AIP Conf. Proc. (1931), https://doi.org/10.1063/1.5024113, 030054-1–030054-7, 2018.
[5] Andi Syahrinaldy Syahruddina, Jalaluddin Jalaluddin, Azwar Hayat, Performance analysis of solar water heating system with plate collector integrated PCM storage, EPI International Journal of Engineering 3 (2) (Aug. 2020) 143–149, https://doi.org/10.25042/epi-ije.082020.09.
[6] D. Ashari, D. Ichsani, Eksperimental study the effect of additional flat plate reflector to performance the sinusoidal solar water heater, IPTEK Journal of Engineering 5 (1) (2019).
[7] N.A. Pambudi, I.R. Nanda, A.D. Saputro, The energy efficiency of a modified v-corrugated zinc-coated steel collector on the performance of solar water heater (SWH), Results in Engineering 18 (2023) 101174.
[8] R. Dobriyal, P. Negi, N. Sengar, D.B. Singh, A brief review on solar flat plate collector by incorporating the effect of nanofluid, Mater. Today: Proc. (2019), https://doi.org/10.1016/j.matpr.2019.11.294.
[9] A. Sakhrieh, A. Al-Ghandoor, Experimental investigation of the performance of five types of solar collectors, Energy Convers. Manag. 65 (2013).
[10] N.I.S. Azha, H. Hussin, M.S. Nasif, T. Hussain, Thermal performance enhancement in flat plate solar collector solar water heater: a review, Processes 8 (2020) 756, https://doi.org/10.3390/pr8070756.
[11] T. Beikircher, P. Osgyan, M. Reuss, G. Strei, Flat plate collector for process heat with full surface aluminium absorber, vacuum super insulation and front foil, Energy Proc. 48 (2014) 9–17.
[12] Y. Selikhov, et al., The study of flat plate solar collector with absorbing elements from a polymer material, Energy 256 (2022) 124677.
[13] B.N. Merzha, M.H. Majeed, F.A. Saleh, Experimental study of flat plate solar collector performance with twisted heat pipe, IOP Conf. Ser. Mater. Sci. Eng. 518 (2019) 032035, https://doi.org/10.1088/1757-899X/518/3/032035.

[14] A.S. Syahruddin, Jalaluddin, A. Hayat, Performance analysis of solar water heating system with plate collector integrated PCM storage, EPI International Journal of Engineering 3 (2) (2020) 143–149.
[15] M.A. Sharafeldin, et al., Evacuated tube solar collector performance using copper nanofluid: energy and environmental analysis, Appl. Therm. Eng. 162 (2019) 114205.
[16] T. Matuska, V. Zmrhal, J. Metzger, Detailed modelling of solar flat-plate collectors with design tool kolektor 2.2, in: 11th International IBPSA Conference, Scotland, 2009, pp. 2289–2296.
[17] H. Vettrivel, P. Mathiazhagan, Comparison study of solar flat plate collector with single and double glazing systems, Int. J. Renew. Energy Resour. 7 (1) (2017).
[18] S. Li, et al., Corrugated transpired solar collectors: mathematical modeling, experimental investigation, and performance analysis, Sol. Energy 262 (2023) 111839.
[19] H. Zhang, et al., Mathematical modeling and performance analysis of a solar air collector with slit-perforated corrugated plate, Sol. Energy 167 (2018) 147–157.
[20] P.K. Pathak, P. Chandra, G. Raj, Experimental and cfd analyses of corrugated plate solar collector by force convection, Energy Sources, Part A Recovery, Util. Environ. Eff. 42 (3) (2020) 304–318, https://doi.org/10.1080/15567036.2019.1587076.
[21] B. Li, et al., Mathematical modeling and experimental verification of vacuum glazed transpired solar collector with slit-like perforations, Renew. Energy 69 (2014) 43–49.
[22] J.P. Holman, Experimental Methods for Engineers, 2012.
[23] J.A. Duffie, W.A. Beckman, Solar Engineering of Thermal Processes, fourth ed., John Wiley & Sons, 2013.
[24] M. Fan, et al., A comparative study on the performance of liquid flat-plate solar collector with a new V-corrugated absorber, Energy Convers. Manag. 184 (2019) 235–248.
[25] N.A. Ogie, I. Oghogho, J. Jesumirewhe, Design and construction of a solar water heater based on the thermosyphon principle, J. Fund. Renew. Energy Appl. 3 (2013), https://doi.org/10.4303/jfrea/235592.